


# Artificial Intelligent Embedded Doctor (AIEDr.): A Prospect of Low Back Pain Diagnosis

Sumit Das, JIS College of Engineering, West Bengal, India

 <https://orcid.org/0000-0002-8018-9151>

Manas Kumar Sanyal, University of Kalyani, Kalyani, India

Debamoy Datta, JIS College of Engineering, West Bengal, India

## ABSTRACT

This article focuses on the development of a diagnostic model for low back pain management, a mathematical model describing the cause of the disease and an inclusive hardware implementation with artificial intelligence (AI). It has been observed that the greater part of the people in developing countries cannot afford the cost of this treatment due to low financial status. Moreover, a continuous assessment is not made for continuous monitoring of the patient's status. The problem of back pain develops slowly and if some early assessments can be made, then the treatment becomes effective. The proposed method developed in this article is based on galvanic skin response (GSR). GSR is used to monitor the pain of the patients and a modified back-pain management algorithm is used for tackling the correlation between stress and pain. The system continuously monitors the condition of a patient and if any symptoms of low back pain (LBP) develop, it immediately diagnoses diseases and chronic pains, and it recommends going to a doctor.

## KEYWORDS

Artificial Intelligence (AI), Galvanic Skin Response (GSR), Low Back Pain (LBP), Mathematical Model of Backbone, Recommendation AUM, Regression Medical Diagnosis

## INTRODUCTION

The major technique of artificial intelligence (AI) have been used in many research papers for diagnosing diseases (Das, Sanyal, & Datta, 2020) but a major problem is that they cannot be implemented in hardware. It is well known that medical diagnosis involves the use of various biosensors, this data needs to be collected from them and

DOI: 10.4018/IJBDAH.2019070103

This article, originally published under IGI Global's copyright on January 17, 2020 will proceed with publication as an Open Access article starting on January 20, 2021 in the gold Open Access journal, International Journal of Big Data and Analytics in Healthcare (converted to gold Open Access January 1, 2021), and will be distributed under the terms of the Creative Commons Attribution License (<http://creativecommons.org/licenses/by/4.0/>) which permits unrestricted use, distribution, and production in any medium, provided the author of the original work and original publication source are properly credited.

as such the conventional techniques of AI like support vector machines (SVM), neural networks (Das, Dey, Pal, & Roy, 2015) become inefficient with the limited memory of the microcontrollers. The physical backbone of a human is modeled with the concept of physics. In the work, an algorithm is proposed that works perfectly in hardware and the main essence of the process is that training is done separately in software and parameters are imported in the hardware to make an embedded doctor that works at any place and any time. The literature survey done in the corresponding section explores the key factor that is important for analysis is the relationship of galvanic skin response (GSR) to pain and correspondingly the method adopted by previous authors in extracting a particular feature from GSR. Then the methodology section is based on a firm mathematical model developed and from that model, the algorithm used for a diagnosis takes the shape, following which the cost-effective method of collecting GSR data is presented along with the schematic diagram and calculations. Finally, the results section is split into two parts one describing the data collected and proposing some hypotheses along with its verification. The second part describes the results of the algorithm proposed. Finally, a conclusion is made regarding the future prospects of this work. The proposed method learns by example from provided data using nonlinear regression. The most interesting fact is that if a low pass filter is used, some of the information that may be present may be lost. Therefore, the algorithm proposed herein works with the unfiltered data but still yields very accurate results and is able to differentiate noise.

## **BACKGROUND**

One most important observation is that when a person feels pain, the stress level of a person also increases. In a paper by Hägni (Hägni et al., 2008), a very important result is obtained as is clear from Galvanic Skin Response to an unexpected threat. This important paper sheds some light that how pain and stress can be related to each other in terms of change in Galvanic Skin Response. Some very interesting researches have been done in Galvanic skin response and how it can measure the stress level of a person. In another paper by Carnagey (Carnagey, Anderson, & Bushman, 2007), the stress levels were analyzed to find the effect of violent video games on a person scientifically. The paper by Huges Farley (Hughes, Farley, & Rhodes, 2010) titled “Vocal and Physiological Changes in Response to the Physical Attractiveness of Conversational Partners” used GSR to determine the effect of voice pitch while talking to attractive people of the opposite sex. In a work by Jan Widacki (Widacki, 2015), it is described as how GSR values can be used to detect lies. The very important observation that comes after studying all these papers is that the way the GSR is used is important in drawing the conclusion. The GSR channel is considered the most diagnostic recording in polygraph examinations, and the best discriminator between people providing deceptive answers to test questions and non-deceptive subjects. Changes in the GSR are still used both for classical polygraph examinations and for a variety of simplified procedures of instrumental lie detection based on the observation

of physiological correlates of emotion (Widacki, 2015). The resistance of the skin will vary depending upon the person's condition. The GUI (Graphical User Interface) can be created in the NI-LabVIEW software program. The GUI uses the protocol NI-VISA, formula node, filtering, Arduino toolkits, waveform viewing, NISound, and Vibration. In a work by Critchley (Critchley, Elliott, Mathias, & Dolan, 2000) an investigation is made regarding functional neuro-anatomy and GSR where they have proved the validity of GSR by linking with the changes in brain activity. Therefore, the used of GSR readings along with flex sensors connected to the lower back of a person are involved for performing the diagnosis. The uses of flex sensors are necessary for diagnosis as is clear from the mathematical model of backbone presented in subsequent sections. In some literature, predict diseases using the concept of self-learning (Das, Sanyal, Datta, & Biswas, 2018) and the term reliability (Das, Sanyal, & Datta, 2018), but this work uses the amalgamation of hardware and software. Therefore, from the literature survey, hypothesize that pain is indirectly related to stress and the stress value can give a measure of pain if appropriate methods are followed.

## METHODOLOGY

### Mathematical Model of Backbone

Muscles, forward flexors, lateral flexors, rotators and extenders are features, which simplify the motion of the x-axis and the angular movement. By considering the L1, L2, L3, L4, L5 to be connected in Figure 1, the writers model the backbone as linking rods; and the torsion-spring models the joints in Figure 1 as shown in Figure 2 in which  $c$  is the spring constant (Bridwell, 2019).

Considering, the range of disks to be  $n$  range of links. Let the joints be approximated as torsion springs that strengthen a torque  $\dot{M} = k\alpha_n$  where  $\alpha_n$  is the angle with the

Figure 1. Lower backbone links ("lumbar-spinal-discs-L1-L2-L3-L4-L5.jpg – Google Search," 2019)

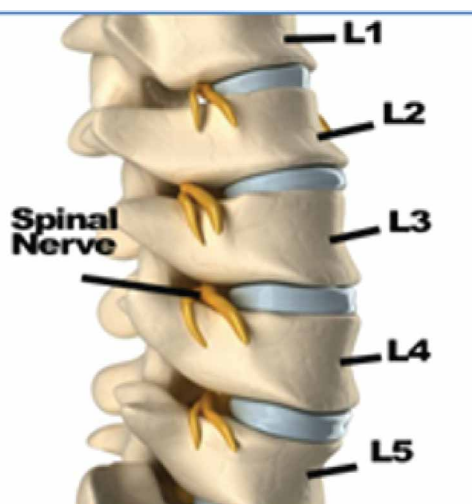
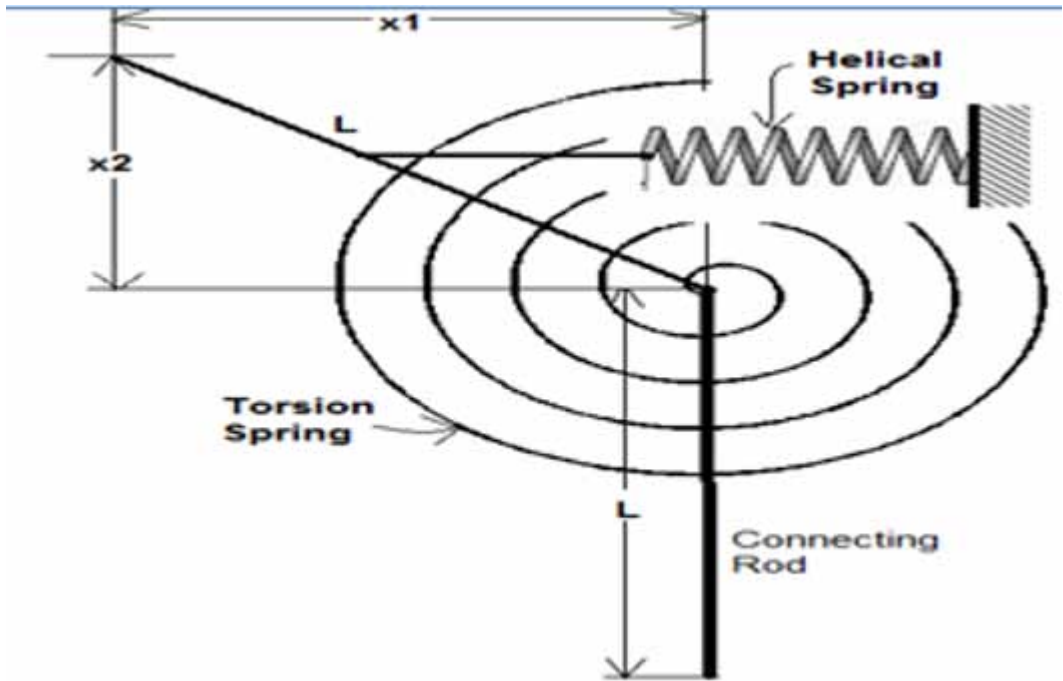


Figure 2. A mathematical model of the backbone



Y-axis. Any fault in the joints will purpose  $\dot{M}_{joint} = 0$  and need to locate the equilibrium circumstance for preventing the joint from buckling below load. For this, the approach of virtual work is used. Consider a virtual displacement of attitude  $d\alpha_n$  is given. From the geometry of the Figure 2 and get Equations 1 and 2:

$$x_1 = l \sin \alpha_n \quad (1)$$

$$x_2 = l \cos \alpha_n \quad (2)$$

Taking differentials on both sides of Equation 1 and 2 and get Equations 3 and 4:

$$x_1 = l \cos \alpha_n \cdot d\alpha_n \quad (3)$$

$$x_2 = -l \sin \alpha_n \cdot d\alpha_n \quad (4)$$

where  $du = 0$ , is the differential change in energy, the above expression is the principle of virtual work:

$$-\frac{m}{n} g \cdot dx_2 - cx_1 dx_1 - M \cdot d\alpha_n = 0 \quad (5)$$

where  $n$  represents the number of links,  $m$  is the mass supported through spine and  $c$  stands for spring constant. Displacement occurs in every-direction. Putting the cost of Equation 3 and 4 in 5, and get:

$$\frac{m}{n} gl \sin \alpha_n \cdot d\alpha_n - cl \sin \alpha_n \cdot l \cos \alpha_n d\alpha_n - M \cdot d\alpha_n = 0$$

By solving, it yields:

$$m = \frac{n}{gl \sin \alpha_n} \left( \frac{1}{2} cl^2 \sin 2\alpha_n + M \right) \tag{6}$$

where,  $M = k\alpha_n t$ .

Therefore, the above Equation (6) becomes:

$$m = \frac{n}{gl \sin \alpha_n} \left( \frac{1}{2} cl^2 \sin 2\alpha_n + k\alpha_n t \right) \tag{7}$$

The spine as described by the Equation (7) can support this mass. The authors have modeled the muscle tissue as springs having spring constant  $c$ . If the patient is struggling from any fault the right-hand facet of the Equation decreases or equivalently announcing the fee of  $m$  turns into more than the equilibrium circumstance for the parameters specified. Now, consider one aspect has modeled the muscle mass as springs having a consistent spring constant. However, the residences of muscle groups fluctuate as the oxygen attention in the blood increases as nicely as the quantity of extension it suffers. Hence, in general, the spring constant  $c$  is a function of both  $x_1$  and  $t$  but earlier than finding out  $c(x_1, t)c(\alpha_n, t)$  let, we locate the oxygen attention in the blood. Now, this is a characteristic of time only, and denotes the amount of oxygen concentration in mg/l of blood with the aid of  $O(t)$ . Now, consider increase the time through  $h$  amount then discover that the awareness of oxygen now and again increases sometimes decreases due to breathing. Another assumption is that oxygen is bump off exponentially with the aid of the muscle cells. By incorporating all the behaviors and get the following Equation:

$$o(t+h) = o(t) - e^{-\gamma h} \sin ah \cdot o(t) \tag{8}$$

The justification of Equation 8, because of the exponentially decaying sinusoidal part finally as  $h$  becomes very large  $O(t+h) \approx O(t)$  or equivalently announcing the concentration of oxygen on a common remains constant. Hence, it is justified in using

the Equation (8), its capability that at the start whatever awareness you had after growing the time it decreases with the aid of a certain fraction of the initial value.

Now, from Equation (8):

$$o(t+h) - o(t) = -e^{-\gamma h} \sin ah$$

or, dividing both sides of the above expression by h, and it yields:

$$\frac{O(t+h) - O(t)}{h} = \frac{e^{-\gamma h} \sin ah}{h} o(t)$$

Now, as limits  $h \rightarrow 0$  the above Equation becomes:

$$\frac{dO(t)}{dt} = ao(t) \tag{9}$$

Hence, the differential Equation has been derived for the concentration of oxygen in the blood. The initial situation  $O(0) = 0$ , solving the underneath Equation 10 and applying the initial condition, and get:

$$o(t) = e^{-ah} - 1 \tag{10}$$

$$\left(\text{Deviation of } c(x_1, t) \text{ in time}\right) \propto \left(\text{Oxygen concentration}\right) \tag{11}$$

$$\left(\text{Deviation of } c(x_1, t) \text{ in time}\right) \propto \left(\text{Deviation of extension of } c(x_1, t)\right) \tag{12}$$

The more the oxygen concentration in blood, additional spring-constant vary with time since more oxygen will produce more energy for the extensions of muscle and it is a common observation that if muscles carry a load for a longer time, fatigue develops in the muscles. Thus, increased extension is possible if the change in muscle extension occurs fast. This is described by the Equation (12).

By combining Equations (11) and (12):

$$\text{Deviation of } c(x_1, t) \text{ in time} \propto \left(\text{Oxygen concentration}\right) \left(\text{Deviation of extension of } c(x_1, t)\right) \tag{13}$$

$$\text{Deviation of } c(x_1, t) \text{ in time} = \frac{c(x_1, t + \Delta t) + c(x_1, t - \Delta t)}{2} - c(x_1, t) \tag{14}$$

Consider a window of  $[+\Delta t, -\Delta t]$  and the first term in the Equation (14), is the average term and subtracting it from  $c(x_1, t)$  and are justified in calling this a deviation of spring-constant in time. Similarly, mathematically define the deviation of the spring constant due to extension. Finally, the Equation (13) becomes:

$$\frac{c(x_1, t + \Delta t) + c(x_1, t - \Delta t)}{2} - c(x_1, t) = k o(t) \frac{c(x_1 + \Delta t, t) + c(x_1 - \Delta t, t)}{2} - c(x_1, t) \quad (15)$$

Here,  $k$  is the constant of proportionality in Equation (15). Dividing both sides of Equation (15) by  $\frac{2}{(\Delta x_1 \Delta t)^2}$ :

$$\begin{aligned} & \frac{2}{(\Delta t \Delta x_1)^2} \left( \frac{c(x_1, t + \Delta t) + c(x_1, t - \Delta t)}{2} - c(x_1, t) \right) \\ &= k o(t) \frac{2}{(\Delta t \Delta x_1)^2} \left( \frac{c(x_1 + \Delta t, t) + c(x_1 - \Delta t, t)}{2} - c(x_1, t) \right) \\ & \frac{2}{(\Delta t)^2} \left( \frac{c(x_1, t + \Delta t) + c(x_1, t - \Delta t)}{2} - c(x_1, t) \right) \\ &= k o(t) \frac{2(\Delta x_1)^2}{(\Delta t \Delta x_1)^2} \left( \frac{c(x_1 + \Delta t, t) + c(x_1 - \Delta t, t)}{2} - c(x_1, t) \right) \end{aligned}$$

At present transform in extension as  $\Delta x_1 \rightarrow 0, \Delta t \rightarrow 0$  the above equation becomes:

$$\frac{\partial^2 c}{\partial t^2} = b o(t) \left( \frac{\partial^2 c}{\partial x_1^2} \right) \quad (16)$$

Hence, got the partial differential equation regarding the change in the spring constant and used the first principle definition of partial derivatives to write Equation (16).

Therefore, got the partial differential equation regarding the alternate in the spring-constant and used the first principle definition of partial derivatives to write Equation (16). Currently outline the preliminary and boundary condition:

$$\lim_{x_1 \rightarrow x_{1 \text{ break}}} c(x_1, t) = q \delta(t) \quad (17)$$

Here  $\delta(t)$  stand for Dirac's delta function; q is the spring-constant parallel to the maximum expansion after which the spring breaks:

$$c(0,0) = 0 \tag{18}$$

$$c(x_1,0) = \xi \tag{19}$$

$$c(0,t) = \varepsilon \tag{20}$$

The Equations (17) through (20) are the limiting conditions of partial-differential Equation.

On behalf of small,  $x_1$  ignore higher order terms in solution and it gives:

$$c(x_1,0) = \varepsilon t^2 + \frac{(\varepsilon + \xi)x_1}{2\sqrt{ae}} e^{\frac{-at}{2}} J_0 \left( -\frac{(a^2 - 2a)}{2} t \right) + \frac{(\varepsilon + \xi)x_1^2}{2ae} \left( \frac{2}{t^2} \delta(t) + \frac{a}{t} \delta(t) \right) + \dots$$

Here  $b = -e$ , assumed  $b$  to be negative. This equation includes Bessel's collection as well as Dirac's delta characteristic has used the technique of Laplace radically change to resolve the equation. Now, the factor is that  $x_1$  can be expressed in terms of  $\alpha_n$ . The intention will become then discovering  $\frac{d\alpha_n}{dm}$  for this differentiate Equation (8) with recognize to and invert the result. This will inform us as  $m$  increases, how the perspective modifications do. Hence, how the whole lot gets affected as the mass to be supported increases. Mathematically decided what takes place and for this reason observed an algorithm that nicely fits and needs for diagnosis. By thinking about all the factors and parameters:

$$c(\alpha_n,t) = \varepsilon t^2 + \frac{(\varepsilon + \xi)l \sin \alpha_n}{2\sqrt{ae}} e^{\frac{-at}{2}} J_0 \left( -\frac{(a^2 - 2a)}{2} t \right) + \frac{(\varepsilon + \xi)(l \sin \alpha_n)^2}{2ae} \left( \frac{2}{t^2} \delta(t) + \frac{a}{t} \delta(t) \right)$$

At this moment differentiating the equation with respect to a  $\alpha_n$  keep other terms as constant, and get:

$$\frac{dc}{d\alpha_n} = \varepsilon t^2 + \frac{(\varepsilon + \xi)l \cos \alpha_n}{2\sqrt{ae}} e^{\frac{-at}{2}} J_0 \left( -\frac{(a^2 - 2a)}{2} t \right) + \frac{(\varepsilon + \xi)l^2 \sin 2\alpha_n}{2ae} \left( \frac{2}{t^2} \delta(t) + \frac{a}{t} \delta(t) \right)$$



Assuming time equal to constant, obtain:

$$\frac{dc}{d\alpha_n} = k_1 + k_2 \cos \alpha_n + k_3 \sin 2\alpha_n \quad (21)$$

In accumulation, after generalization of derivative of Equation (8) with respect to  $\alpha_n$  and inverting the results and using Equation (21):

$$\frac{dc}{dm} = \frac{gl}{n \left( l^2 k_1 (\cos \alpha_n - \sin \alpha_n) + l^2 k_2 (\cos^2 \alpha_n - \sin^2 \alpha_n) + l^2 k_3 (\sin 2\alpha_n \cos \alpha_n - \sin^3 \alpha_n) \right)} \quad (22)$$

At present, result in Equation 22 is periodic in character namely the value varies between  $q_1$  and  $q_2$  and if  $l$ ,  $n$ , and  $t$  remains unchanged.

So,  $\left( \frac{d\alpha_n}{dm} \right)_{avg} = constant$ , consequently get a startling fact that on an average if  $t$

remains constant, the angle changes at a regular rate. If  $t$  increases, the change of perspective with the alternate in mass will be decreased. Thus, weight problems will no longer be a reason of LBP. Now, due to some reasons, one or extra of the links are no longer working properly. The case for spondylitis is particularly identical the place few links do no longer work. In such a case:

$$\frac{dc}{dm} \propto \frac{1}{n} \quad (23)$$

As it has been seen from Equation 23 as  $n$  decreases  $\frac{d\alpha_n}{dm}$  increases, which potential from even a small trade in mass the change in angle is very massive and as a result the joint may get disrupted. Similarly, it is more possibly that a joint failure might also manifest in other parts of the body, as length per unit link is large. Now, if the perspective crosses a certain restriction then it is possibly that the joint will be damaged. Therefore, the aspect in Equation (22) is very essential as can be considered in the following sections.

### Development of Diagnostic Algorithm From the Mathematical Model and GSR

From the Equation (22), and get:

$$\frac{d\alpha_n}{dm} \approx \frac{gl}{n \left( l^2 k_1 (1 - \alpha_n) \right)}$$

As for small values of  $\alpha_n$ ,  $\cos(\alpha_n)$  approximately 1 and  $\sin(\alpha_n)$  approximately becomes  $\alpha_n$ . Consequently, the above Equation becomes:

$$\frac{d\alpha_n}{dm} \approx \frac{c}{(1-\alpha_n)} \quad (24)$$

The Equation 24 forms the main basis of the proposed Algorithm 1.

#### Algorithm 1. Proposed algorithm

1. Calculate FFT of the signal.
2. Input flex sensor voltage
3. Calculate  $\alpha_n$
4.  $m = \alpha_n - \alpha_{n-1}$
5. if ( $m > b_1$ )
  - a. count++
  - b. end
6. if ( $a_1 < \frac{c}{1-\alpha_n} < a_2$ )
  - a. Display "you are healthy keep it up" Go to step 1.
  - b. end
7. Declare  $R = const + B * \sin(A * n) + const2 * x + const3 * \left(\frac{1}{x}\right)$  where the last term is optional and a nonlinear regression model is trained  $pr(>|t|)$  values are extracted for each constant.
8. Define  $z = constant * \log(1/pr(>|t|))$  where the constant is the value obtained after regression for the first constant it is called as the stress, for A it is called the  $z_{\text{chanting/movement}}$  for const2 the z value is multiplied with first z value defined for the first constant and that z is called  $z_{\text{pain}}$ .
9. if ( $count \leq 4 \mid \mid \frac{c}{1-\alpha_n} < \xi_2$ )
  - a. if ( $z_{\text{pain}} \leq \varepsilon_1 \ \&\& \ m < \varepsilon_2$ )
    - i. display ("are you sitting?")
    - ii. input (op)
    - iii. if (op=='y')
      1. display ('you are suffering from Herniated Neucleas Polpusus')
      2. break
      3. end
    - iv. if (op=='n')

```
    1. display ('you are suffering from spinal stenosis')
    2. break
    3. end
v. Display ('if you are sitting stand and vice versa?')
vi. If ( $z_{pain} \leq \varepsilon_3$ )
    1. Display ('you are suffering from compression fracture')
    2. break
    3. end
vii. display ('enter your weight')
viii. input(q)
ix. if(35-q<10)
    1. display ('bone cancer suspected')
    2. break
    3. end
x. end
b. else
    i. display ('do some exercise')
    ii. end
10. if(count > 4)
    a. if ( $z_{exercise} < \varepsilon_4$ )
        i. display ('sufficient exercise done')
        ii. count=0
        iii. break
        iv. end
    b. else
        i. display ('do more exercise')
        ii. end
11. if (FFT_low_frequency_present())
    a. display ('Good do more meditation')
    b. break
    c. end
12. if (FFT_high_frequency_present())
    a. display ('please do meditation')
    b. end
13. end
```

The advantage of this algorithm is that it can be effectively implemented in a microcontroller as training is done outside the microcontroller and only the required parameters obtained from Support Vector Machines are fed to the microcontroller for analysis. Now,  $\frac{d\alpha_n}{dm}$  parameter is very crucial because it ultimately indirectly gives the load-bearing capacity of the backbone. So, in case of faults in the backbone, the value of this variable would change first and hence this is incorporated in the algorithm.

Under different conditions, GSR varies so different model parameters need to be used to get accurate results.

### Simulated Diagram for Collecting of Data

The hardware that is used for building the circuit involves, BC547 transistors, Arduino Uno, 100-ohm resistors and 50-ohm resistors were used instead of 10-ohm along with analog type flex sensor (Figure 3). The reason for choosing this setup is cost effectiveness. The cost of a BJT (Bipolar Junction transistor) is 0.01 dollars approximately. Thus, it can be implemented very easily at any place and is effective for commercialization. The Arduino microcontroller has been chosen for its simplicity although this entire process can be implemented in any microcontroller of choice after proper calibration as described in the algorithm. Various Darlington pair IC are available in the market that if used can further reduce the cost as well as improve the reliability and durability of the setup.

### Propose Hardware Model Flow Diagram

See Figure 4.

### Calculations of GSR

From the circuit, the base current into the first transistor is given by:

$$i_b = \frac{5 - v_{be}}{R_{skin}} \tag{25}$$

Figure 3. Schematic diagram for the measurement of GSR and flex sensor values

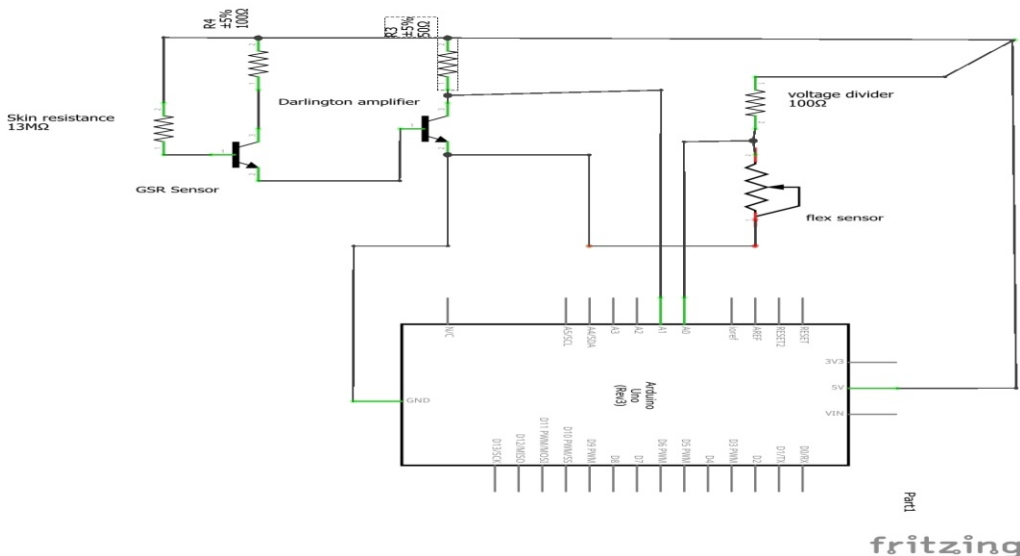
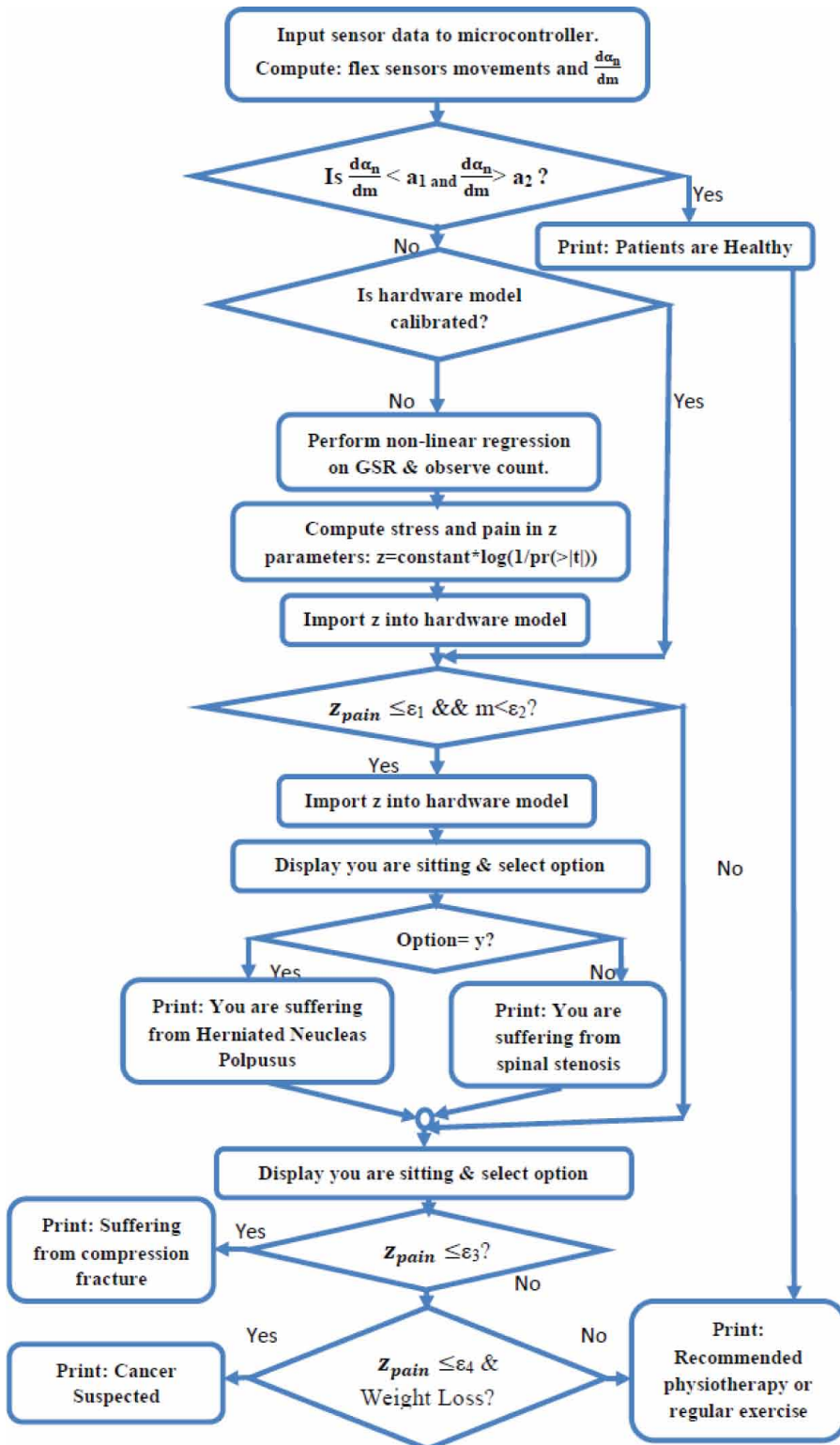


Figure 4. Flow diagram of *Propose Hardware Model*



Nevertheless,  $v_{be}$  for the transistor is  $0.7v$ . Thus, Equation 25 becomes:

$$i_b = \frac{4.3}{R_{skin}}$$

Therefore, the current flowing through the collector of the second transistor is given as:

$$i_c = \beta^2 i_b \tag{26}$$

However, collector current can be measured as:

$$i_c = \frac{5 - v_{ce}}{50}$$

Putting this in (25) yields:

$$\frac{5 - v_{ce}}{50} = \beta^2 i_b$$

or, by the Equation (26) and get:

$$\frac{5 - v_{ce}}{50} = \beta^2 \frac{4.3}{R_{skin}}$$

In this case  $v_{ce}$  is input to the analog pin of Arduino. The above equation becomes:

$$R_{skin} = \frac{\beta^2 \times 50 \times 4.3}{5 - v_{A1}}$$

Here, the  $\beta = 368$  as BC547 transistor is used, after all, calculations the value of GSR comes out to be:

$$R_{skin} = \frac{29.11616}{5 - kv_{measured}} M\Omega \tag{27}$$

The k comes because Arduino represents 5V by number 1023. Another type of GSR was used which called as scaled GSR where the k is assumed to be 1. This result was used for one sample of data collected and it was studied:

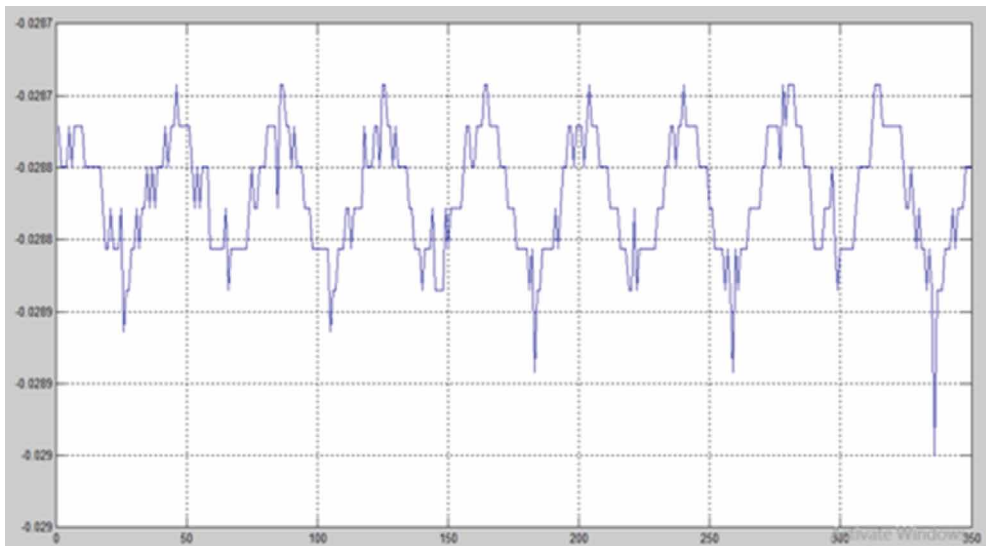
$$R_{skinscaled} = \frac{29.11616}{5 - v_{A1}} M\Omega \quad (28)$$

where  $k = 1$  for the first data shown in Figure 6 that collected and for subsequent data Equation (28) was used. Following Figure 5 is showing a sample data acquiring process.

Figure 5. Showing the method of data collection of GSR



Figure 6. Showing the readings of scaled GSR, when the person is stressed



## Result and Analysis

The data collected from the Arduino is imported to MATLAB by serial communication. The observations were made for two minutes and the data were verified and double-checked. Then graphs of GSR along with the observation number on the x-axis were made.

This result shows that when the stress level of a person increases then the skin resistance decreases as sweat glands become active and the signals are sent to them by the Central nervous system. Figure 6 is that of test subject1 who was asked to do tension for 2 minutes during which the reading was taken.

Another interesting phenomenon is that a person gets relaxed a bit when he/she breathes deeply. This common exercise recommended to people undergo through anxiety and depression. The readings were taken while the second subject was breathing deeply, as can be seen from the results that the GSR is high. This implies that the person becomes much relaxed when doing this exercise.

Next, the data is collected when the subject is told to do tension, as is clear from Figure 8 the GSR value has decreased considerably, indicating clearly that the person is tensed. Previously in Figure 7, it was close to 50 M $\Omega$  but in Figure 7, it has been seen that it is close to 35 M $\Omega$ .

It has been the belief in the religion that doing meditation improves the overall ability of a person, to test the fact the subject was asked continuously chant AUM for 2 minutes while recording the data. In each of the graphs that were obtained, a very low frequency sinusoidal component was present. Figure 9 itself shows that it is a modulation of a low-frequency component and upon it, noise and other harmonics are imposed.

Figure 7. The GSR readings during deep breathing

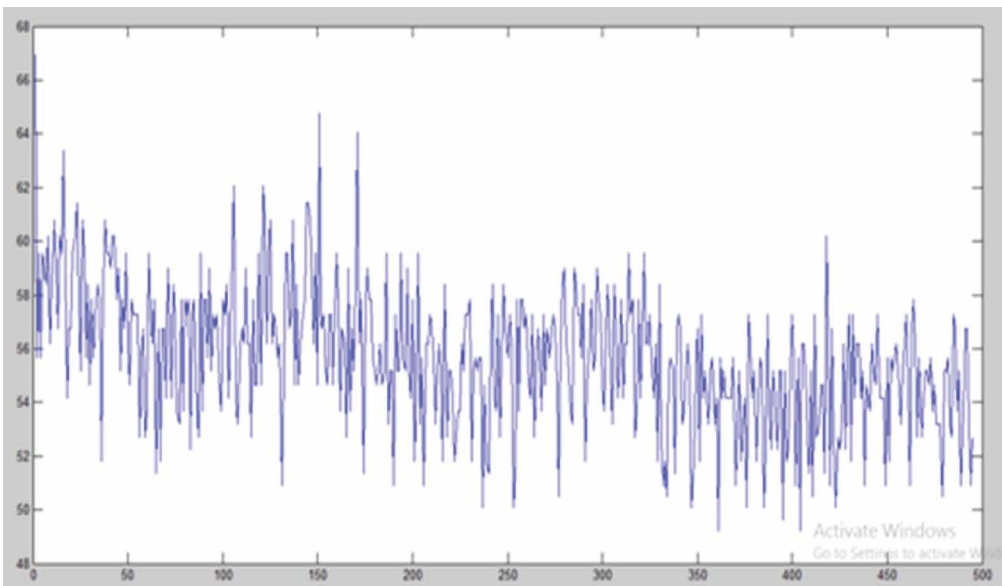




Figure 8. Showing the plot of GSR under tensed

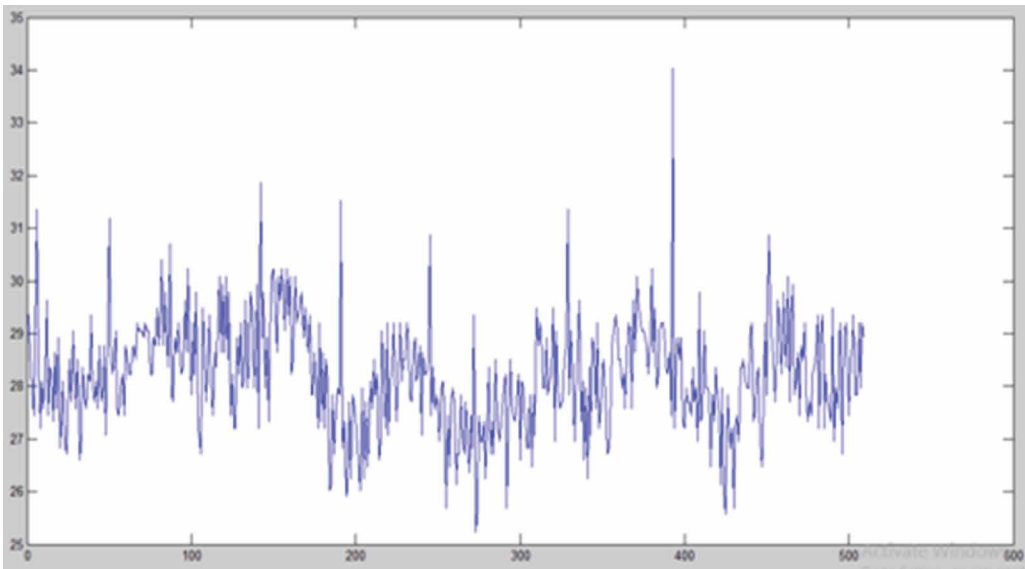
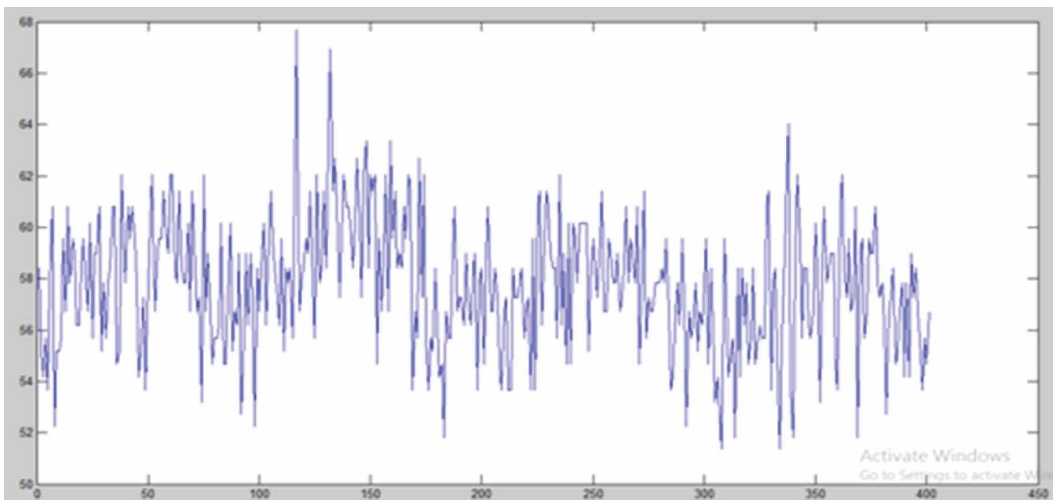


Figure 9. Effect of chanting AUM



So, another figure is given as a verification of the results, Figure 12 still has a low-frequency sinusoidal component as would be clear from the next result section however along with the low frequency another thing is that GSR decreases as the subject later confessed he was a bit tense at that time. In fact, this low frequency nearly matches the frequency of pronouncing “AUM”. Meditations involving some sacred words are common to most religious people and this result confirms the fact that some interesting phenomena occur inside the body during chanting. The works regarding the chanting of AUM using has been done using GSR (Das & Anand, 2012). However, in the case

of low back pain management would recommend meditation whenever required. The paper (Das & Anand, 2012) actually supports the model.

After a lot of experiments, it has been observed that rigorous movements cause more fluctuations in GSR. The overall value of GSR decreases and this is confirmed in various works of literature (Westeyn, Presti, & Starner, 2016). A logical explanation for this would be that even doing small exercise stimulates the sweat glands and conductivity of skin increases a little as a result GSR decreases. In Figure 10 and Figure 11 the noise levels are different, but the characteristics are same and the values in the y-axis clearly show that the effect of stress is clearly observable in values regardless of any muscle movement.

Figure 10. Muscle movement when relaxed

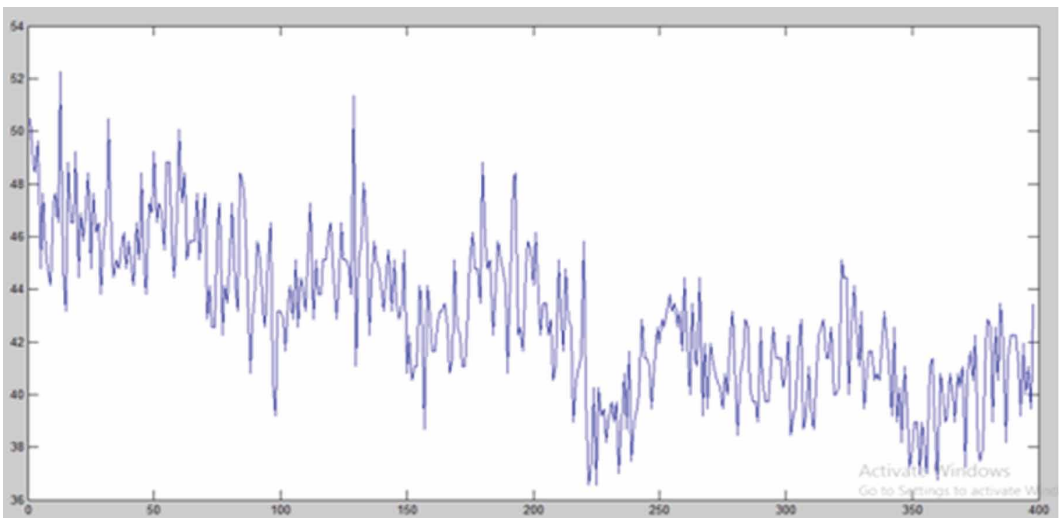


Figure 11. Muscle movement when not relaxed

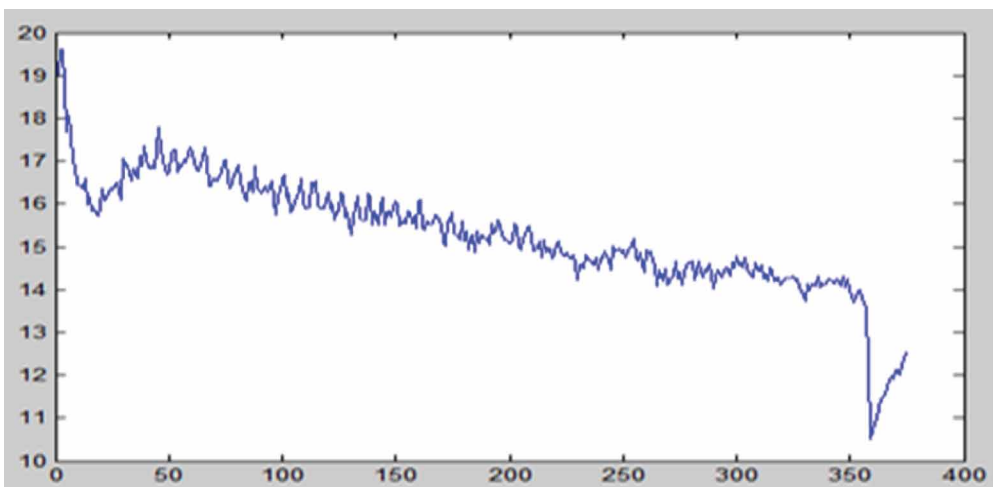
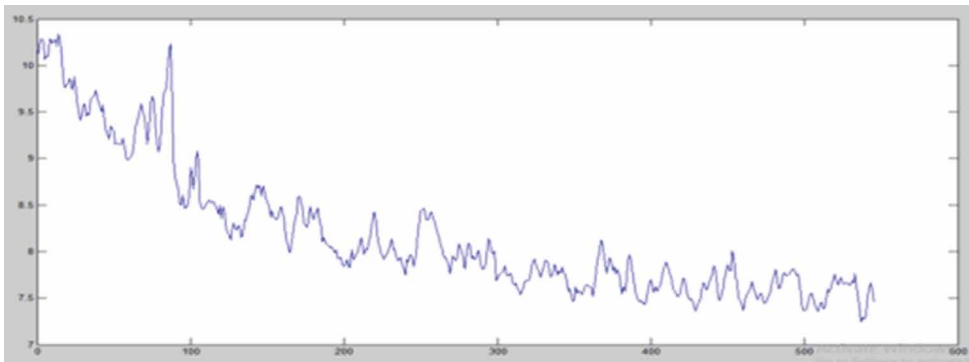


Figure 12. Effects of chanting AUM second reading for verification



## RESULTS OF REGRESSION

In the algorithm, a nonlinear regression model is to be obtained. So, to do this the data is imported from MATLAB to R using the library R.matlab (Bengtsson, 2018) (Figure 13).

Here the value of A is very significant as is obtained from the t values and the  $pr(>|t|)$  column. It is nearly 1 indicating the presence of low-frequency component thus confirming the hypothesis that during the chanting of “Aum” a low-frequency component would always be present. In the first look Figure 12 appears to contradict the assumption but on analysis, as it has been seen in Figure 14, the frequency component is dominant. Figure 14 shows various parameters associated with the nonlinear regression.

Again, as can be seen from Figure 15, the value of the constant A is significant, and A is approximately 2. With a standard error of 0.014 indicating that the frequency component is high, and that A cannot fully account for the observation because of the noise. The value of the first term in the formula used for linear regression is 17.24, significantly higher than that of the results of Figure 14, indicating GSR, in this case, is

Figure 13. The results of nonlinear regression applied to the corresponding data of Figure 11

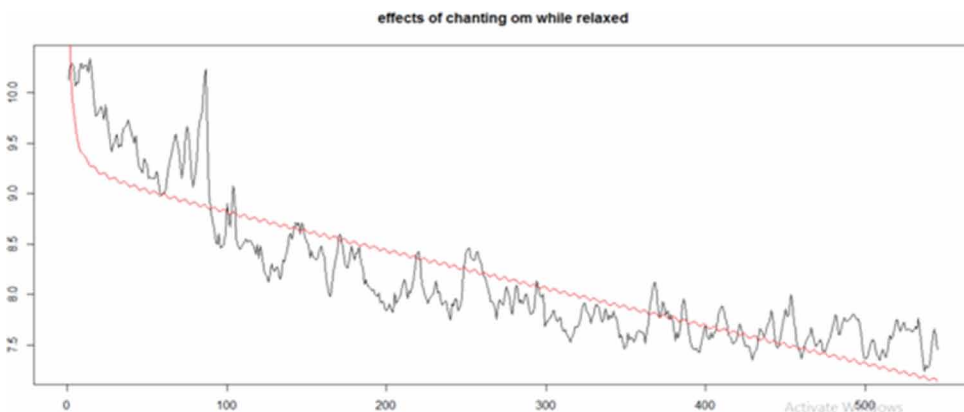
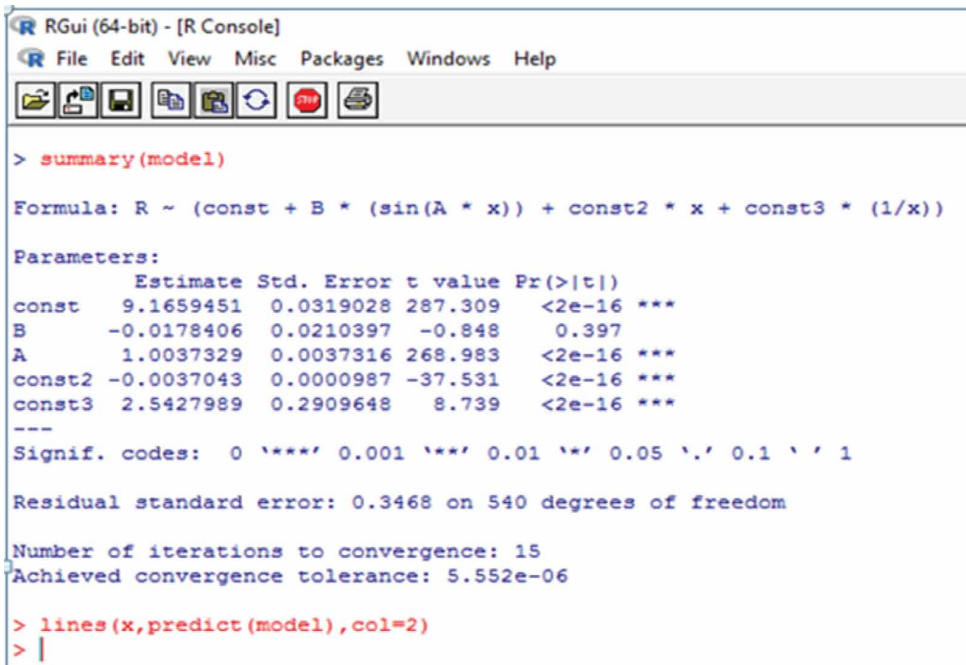


Figure 14. The results of the nonlinear regression on the data corresponding to Figure 11



```
RGui (64-bit) - [R Console]
File Edit View Misc Packages Windows Help

> summary(model)

Formula: R ~ (const + B * (sin(A * x)) + const2 * x + const3 * (1/x))

Parameters:
      Estimate Std. Error t value Pr(>|t|)
const  9.1659451  0.0319028 287.309  <2e-16 ***
B      -0.0178406  0.0210397  -0.848  0.397
A       1.0037329  0.0037316 268.983  <2e-16 ***
const2 -0.0037043  0.0000987 -37.531  <2e-16 ***
const3  2.5427989  0.2909648   8.739  <2e-16 ***
---
Signif. codes:  0 '***' 0.001 '**' 0.01 '*' 0.05 '.' 0.1 ' ' 1

Residual standard error: 0.3468 on 540 degrees of freedom

Number of iterations to convergence: 15
Achieved convergence tolerance: 5.552e-06

> lines(x, predict(model), col=2)
> |
```

high and the person is stressed. Const2 is small but negative indicating GSR decreases slowly if it is compared this with the values obtained in Figure 14; the rate of decrease is more. This is easily interpreted as some physical exercise is taking place. Thus, the key observation is that these small changes in the value of constants obtained from the results can indicate the condition of the patient, accurately.

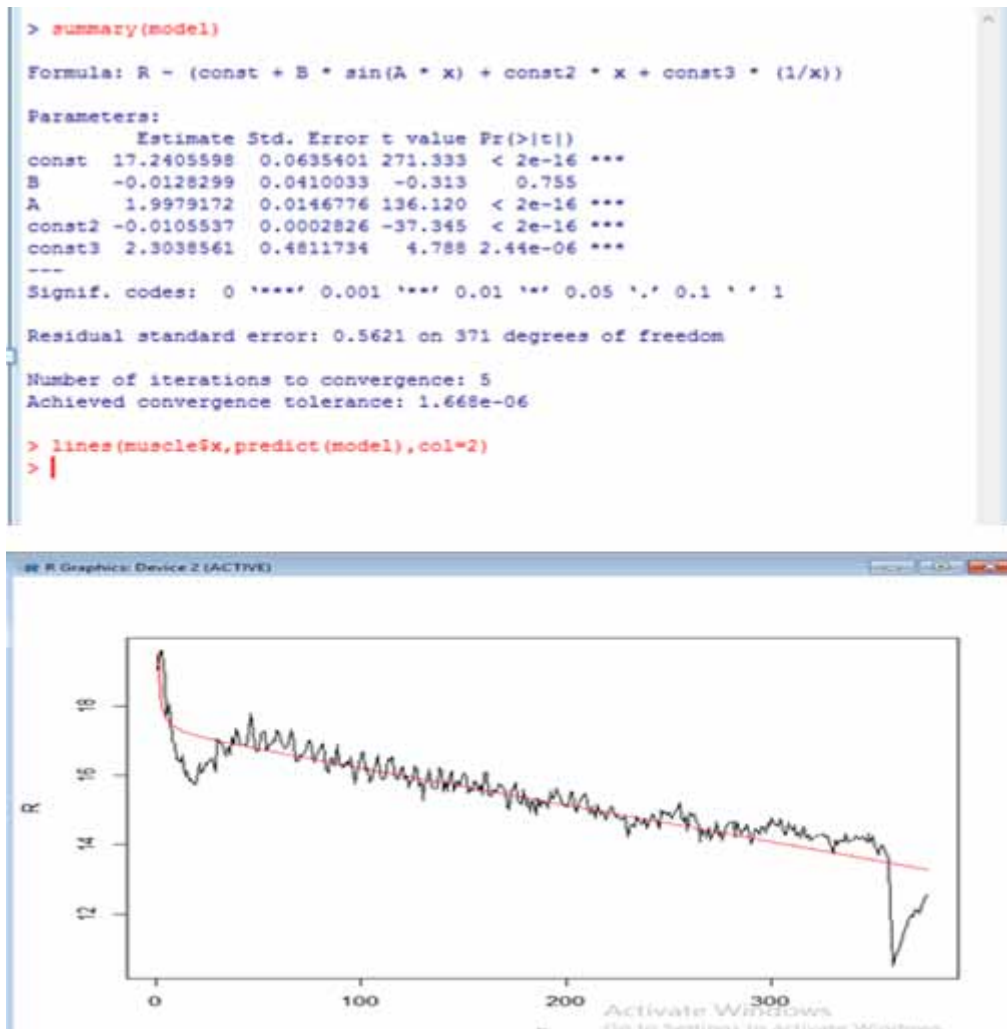
Key findings in comparison to the previous work (Das, Sanyal, & Datta, 2019):

- The amount of pain in a person is directly proportional to the stress and a scientific measure of that is galvanic skin resistance;
- Under various conditions, GSR value changes like doing exercise;
- Thus, all changes in the body can be monitored and this is effectively utilized in developing the diagnostic algorithm.

## CONCLUSION

The work started with an aim to develop a simple yet accurate solution for the diagnosis of low back pain using embedded technology and a new algorithm has been proposed for the low back pain diagnosis. The GSR has been utilized for precise analysis of the disease and the GSR recording sensor developed is very simple yet effective in drawing the conclusion. In developing the work, some interesting phenomena have been observed regarding meditation and chanting of the sacred word of Hindus “AUM.” In fact, apart from reducing stress, a harmonic component has been observed.

Figure 15. Showing the results of nonlinear regression on data of Figure 11



In future work, the incorporation of fuzziness in the algorithm would increase the accuracy even many times. Further, more complex nonlinear model may be used with the algorithm to yield extremely high accuracy. There is a scope of using the Genetic Algorithm to find the minimum value of galvanic skin resistance under different constraints and conditions.

## ACKNOWLEDGMENT

Our thanks to the experts Dr. (Prof.) Manas Kumar Sanyal, University of Kalyani, who have advised and encouraged us for such kind of development. In addition, our special thanks to our Management, JIS College of Engineering, JIS GROUP for providing all kinds of required resources and facilities.

## REFERENCES

- Bengtsson, H. (2018). Read and Write MAT Files and Call MATLAB from Within R [R package R.matlab version 3.6.1]. Retrieved from <https://CRAN.R-project.org/package=R.matlab>
- Bridwell, K. (2019). Spinal Muscles: A Comprehensive Guide. Spine Universe. Retrieved from <https://www.spineuniverse.com/anatomy/spinal-muscles-1>
- Carnagey, N. L., Anderson, C. A., & Bushman, B. J. (2007). The effect of video game violence on physiological desensitization to real-life violence. *Journal of Experimental Social Psychology*, 43(3), 489–496. doi:10.1016/j.jesp.2006.05.003
- Critchley, H. D., Elliott, R., Mathias, C. J., & Dolan, R. J. (2000). Neural Activity Relating to Generation and Representation of Galvanic Skin Conductance Responses: A Functional Magnetic Resonance Imaging Study. *The Journal of Neuroscience*, 20(8), 3033–3040. doi:10.1523/JNEUROSCI.20-08-03033.2000 PMID:10751455
- Das, I., & Anand, H. (2012). Effect of Prayer and “OM” Meditation in Enhancing Galvanic Skin Response. *Psychological Thought*, 5(2). doi:10.5964/psycet.v5i2.18
- Das, S., Dey, A., Pal, A., & Roy, N. (2015). Applications of Artificial Intelligence in Machine Learning: Review and Prospect. *International Journal of Computers and Applications*, 115(9), 31–41. doi:10.5120/20182-2402
- Das, S., Sanyal, M., Datta, D., & Biswas, A. (2018). AISLDr: Artificial Intelligent Self-learning Doctor. In V. Bhateja, C. A. Coello Coello, S. C. Satapathy, & P. K. Pattnaik (Eds.), *Intelligent Engineering Informatics* (pp. 79–90). Springer. doi:10.1007/978-981-10-7566-7\_9
- Das, S., Sanyal, M. K., & Datta, D. (2018). Advanced Diagnosis of Deadly Diseases Using Regression and Neural Network. In J. K. Mandal & D. Sinha (Eds.), *Social Transformation – Digital Way* (pp. 330–351). Springer. doi:10.1007/978-981-13-1343-1\_29
- Das, S., Sanyal, M. K., & Datta, D. (2019). Intelligent Approaches for the Diagnosis of Low Back Pain. In *Proceedings of the Amity International Conference on Artificial Intelligence (AICAI)*. IEEE Press. Retrieved from <https://ieeexplore.ieee.org/document/8701266>
- Das, S., Sanyal, M. K., & Datta, D. (2020). Artificial Intelligent Reliable Doctor (AIRDr.): Prospect of Disease Prediction Using Reliability. In J. K. Mandal & D. Sinha (Eds.), *Intelligent Computing Paradigm: Recent Trends* (pp. 21–42). Springer. doi:10.1007/978-981-13-7334-3\_3
- Hägner, K., Eng, K., Hepp-Reymond, M.-C., Holper, L., Keisker, B., Siekierka, E., & Kiper, D. C. (2008). Observing Virtual Arms that You Imagine Are Yours Increases the Galvanic Skin Response to an Unexpected Threat. *PLoS One*, 3(8), e3082. doi:10.1371/journal.pone.0003082 PMID:18769476

Hughes, S. M., Farley, S. D., & Rhodes, B. C. (2010). Vocal and Physiological Changes in Response to the Physical Attractiveness of Conversational Partners. *Journal of Nonverbal Behavior*, 34(3), 155–167. doi:10.1007/s10919-010-0087-9

Westeyn, T., Presti, P., & Starner, T. (2016). ActionGSR: A combination galvanic skin response-accelerometer for physiological measurements in active environments. In *Proc. 10th IEEE Int. Symp. on Wearable Computers* (pp. 11–14). IEEE Press.

Widacki, J. (2015). Discoverers of the Galvanic Skin Response. *European Polygraph*, 9(4), 209–220. doi:10.1515/ep-2015-0008

*Sumit Das is presently working as an Asst. Professor in the Department of Information Technology, JIS College of Engineering, West Bengal, India. He completed his M.Tech degree in Computer Science and Engineering from the University of Kalyani in the year 2008.*

*Manas Kumar Sanyal is a professor and former Dean of the Faculty of Engineering, Technology and Management, Kalyani University.*

*Debamoy Datta is a student of the JIS College of Engineering, Department of Electrical Engineering.*